Random vibration fatigue with non-stationary loads using an extended fatigue damage spectrum with load spectra

P. Wolfsteiner, A. Trapp, L. Fertl
University of Applied Sciences Munich, Department 03
Dachauerstr. 98b, 80335 Munich, Germany
e-mail: **peter.wolfsteiner@hm.edu**

Abstract
Assessing the fatigue damage potential of vibration loading imposed on vibratory structures can be very demanding. Often, reproducing realistic load conditions in simulations or experiments is almost impossible, especially for non-stationary or non-Gaussian random vibration loading. A common solution is the replacement of recorded loads by simplified definitions – such as Gaussian loads – offering tremendous advantages. Very popular is the Fatigue Damage Spectrum (FDS) as a measure for assessing fatigue damage equivalence. Its model reduces a complex response behavior of real structures to single vibration modes and employs a simple fatigue damage hypothesis. Applying this concept for deriving Gaussian loads can lead to significant deviations of the response load spectra and consequently to the fatigue damage as well. This paper proposes a solution to this issue by i) introducing an enhanced FDS which uses load spectra as fatigue damage measures and ii) by using multiple instead of single Gaussian load definitions.

1 Introduction

A fatigue assessment is a challenging issue for engineers if loads are random and if loaded structures show a distinct dynamical behavior. Despite ongoing research activities, there are no comprehensive methods available – especially for non-Gaussian loading – that are generally applicable to the needs of numerical and experimental fatigue analyses. While a theoretical framework based on power spectral densities (PSD) is well developed and offers powerful capabilities for simulations and experiments, its theoretical foundation is limited to Gaussian random loading. An application of these methods for non-Gaussian loading may cause serious, non-conservative deviations of the predicted fatigue damage. To overcome these issues a variety of approximative methods have been developed. A consideration of the non-Gaussian probability density (expressed by the kurtosis), in addition to the PSD, was suggested for simulations [1, 2] and experiments [3–5]. Further, [6, 7] proposed a procedure based on the model of an amplitude-modulated Gaussian load, using the modulating function to determine the impact on the vibrational response of a structure. But a central issue of all these methods is the question of how the kurtosis of the excitational load transfers to the kurtosis of the response stresses [8]. Recently, this question has been analyzed by [9, 10] based on the theory of higher order spectra. On the basis of this theory, a procedure is proposed for decomposing non-Gaussian loads into a series of Gaussian loads having the equivalent fatigue potential [11–13].

Another considerably simple and thus popular method for analyzing the fatigue damage potential of arbitrary – e.g. non-Gaussian – random vibration loading is the Fatigue Damage Spectrum (FDS). A detailed introduction has been given in [14]. The FDS models a virtual vibratory structure by using the fundamental hypothesis, that even if an arbitrary structure has multiple resonant frequencies its fatigue response behavior is dominated by individual vibration modes. The corresponding model uses a parametric single-degree-of-freedom (SDOF) vibratory system with a variable natural frequency. Varying that natural frequency and evaluating the corresponding fatigue damage provides a meaningful representation of the vibration modes the load excites. The resulting FDS plot depicts the load's fatigue damage potential over the natural frequencies of the virtual structure. Hereby the FDS enables comparing different vibration loads in terms of

its fatigue damage potential for a desired range of frequencies. As a consequence, the FDS can be applied for obtaining synthetic substitute loads – mostly PSD based – that aim to replicate the fatigue damage potential of the referencing original non-Gaussian load. Because of the concept's simplicity, it has gained wide popularity and found a variety of applications. Different calculation approaches of the FDS are studied in [15]. A combination of deterministic and random excitation signals (sine-on-random) is analyzed in [16]. The FDS has been used to assess the fatigue damage potential of multiple PSDs [17], of shock response spectra (SRS) and also for deriving equivalent vibration loads for shaker tests [18]. The limits of the validity of the FDS are investigated in [19] using higher order spectra. As PSD-based load definitions offer important advantages for simulations and experiments, FDS-based procedures for deriving these PSDs are described on a theoretical base e.g. in [14] and also in standards for shaker test [20]. Publications [21, 22] propose further improvements and detailed procedures. A combination with shock response spectra and a comparison with other simplified methods is presented in [23, 24].

Despite its simplicity, the FDS method compromises a set of limitations. A critical issue is, that for the FDS one must define a fatigue damage hypothesis (e.g. Palmgren-Miner rule) which needs at least one slope parameter k even in its very simple single slope version. As a consequence, the validity of damage-equivalent loads derived according to the FDS is restricted to this hypothesis and the specific slope k. This being said, typically the value of k is not constant for one component or an assembly, because its distinct value depends on various aspects like material, surface, character of notch, tempering and others. Especially for a shaker test with an assembly of different parts, it is impossible to adjust to a meaningful value of k. The objective of this paper is to overcome this issue by proposing an alternative definition of the FDS. The FDS' representation is extended from scalar damage values (under the specific damage rule) to the load spectra of all SDOF systems' responses. To further enable an approximation of these load spectra by PSD-based load definitions, we propose to use a definition with multiple (quasi-stationary load) instead of a one single PSD (e.g. see [12, 13, 25, 26]). The following material presents that concept and a procedure for the derivation of this set of PSDs. Its presentation is based on synthetically generated non-Gaussian loads as well as on loads from real application. The following Section 2 provides some background of the study of non-Gaussian random loading, the FDS and its corresponding challenges. Section 3 presents the improved method based on a synthetically generated non-Gaussian load. Finally, Section 4 applies the proposed method to real data. Lastly, this paper ends with conclusions.

2 Random signals and vibration fatigue

2.1 Gaussian and non-Gaussian signals

Stationary Gaussian signals $x_g(t)$ follow the central limit theorem (CLT). Their probability density function (PDF) $p_g(x)$ is fully defined by mean μ_x and standard deviation σ (with $\mu_2 = \sigma^2$).

$$p_g(x) = \frac{1}{\sqrt{2\pi\sigma^2}} e^{\left(-\frac{(x-\mu_x)^2}{2\sigma^2}\right)} \tag{1}$$

whereby $\mu_x = m_1$ and σ can be derived from the general equations for moments m_n and central moments μ_n:

$$m_n = \mathrm{E}[X^n(t)] = \int_{-\infty}^{+\infty} x^n\, p(x)\, dx\,; \qquad \mu_n = \mathrm{E}[(X(t) - \mathrm{E}[X(t)]^n)] = \int_{-\infty}^{+\infty} (x-\mu_x)^n\, p(x)\, dx \tag{2}$$

The definition in the frequency domain is based on the PSD $G_{xx,g}(f)$; the relationship to the time domain representation $x_g(t)$ is given by:

$$\mu_2 = \sigma^2 = \int_0^{\infty} G_{xx,g}(f)\, df \tag{3}$$

allowing a robust synthetic generation of Gaussian stationary signals according to the CLT. Non-Gaussian signals $x_{ng}(t)$ do not follow the CLT and show a PDF $p(x_{ng})$ deviating from its Gaussian analogue $p_g(x)$. A common measure to quantify this deviation is the kurtosis defined by $\beta = \mu_4/\mu_2$; the corresponding Gaussian value is $\beta_g = 3$. For the synthetic generation of non-Gaussian signals there is a wide variety of

methods that have been proposed. The following presentation makes use of a specific non-stationary random excitation signal $x_{ng}(t)$ consisting of a sequence of stationary Gaussian processes (quasi-stationary) [12, 13]. Here a sequence of two processes $x_{g1}(t)$ and $x_{g2}(t)$ with different PSDs $G_{xx,g1}(f)$ and $G_{xx,g2}(f)$ as well as different durations T_1 and T_2 are used. The underlying model approximates a modulation process with an evolution in time and frequency [13]. Figure 1 shows the corresponding PSDs in (a) and the composed time signal $x_{ng}(t)$ in (e). In addition the average PSD $G_{xx,ng}(f)$ of signal $x_{ng}(t)$ is also depicted in (a); the corresponding Gaussian signal $x_g(t)$ with a PSD $G_{xx,g}(f) \approx G_{xx,ng}(f)$ is shown in (d). (c) depicts the PDFs of $x_g(t)$ and $x_{ng}(t)$ with a kurtosis value of $\beta_{ng} = 4$ for the non-Gaussian signal. The PSDs $G_{xx,ng1}(f)$ and $G_{xx,ng2}(f)$ follow a specific definition for the different frequency intervals $[10\ \text{Hz}, 30\ \text{Hz}]$, $[30\ \text{Hz}, 50\ \text{Hz}]$, $[50\ \text{Hz}, 80\ \text{Hz}]$ and $[80\ \text{Hz}, 90\ \text{Hz}]$ to develop different frequency related degrees of non-stationarity.

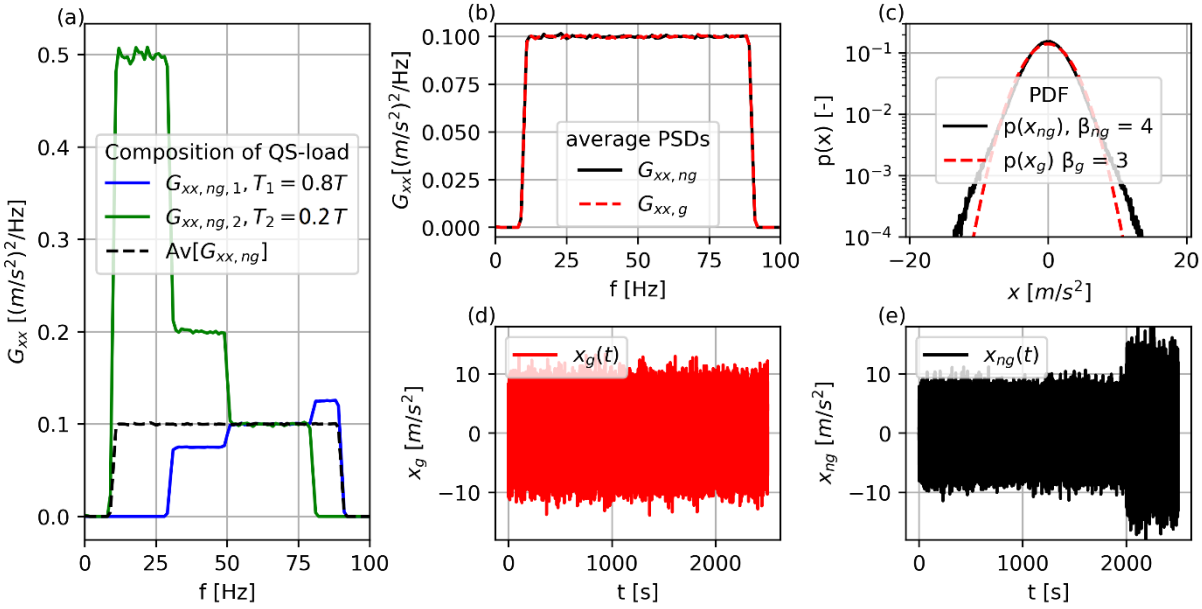

Figure 1: synthetically generated Gaussian and non-Gaussian excitation signals. (a) PSDs $G_{xx,ng1}(f)$ and $G_{xx,ng2}(f)$ of a sequence of stationary Gaussian processes and average PSD $G_{xx,ng}(f)$; (b) PSDs of average PSD $G_{xx,ng}(f)$ and corresponding PSD $G_{xx,g}(f)$ of Gaussian process; (c) PDFs; (d) time realization of $x_g(t)$; (e) time realization $x_{ng}(t)$ with $T_1 = 2000$ s and $T_2 = 500$ s.

2.2 Fatigue Damage Spectrum (FDS)

The Fatigue Damage Spectrum (FDS) [14] is a measure for assessing the fatigue damage potential of vibration loading acting on arbitrary vibratory structures. It can be applied to any kind of load types, like stationary or non-stationary, deterministic or random, Gaussian or non-Gaussian but also any kind of mixed loading. The FDS models a virtual vibratory structure by using the hypothesis of single dominant vibration modes relevant for its fatigue response behavior, even if the original structure has multiple resonant frequencies. The fatigue damage caused by a single vibration mode represents the relevant fatigue measure. Based on this measure (here: $y_{\text{equ}}(f_D)$) the fatigue damage potential of vibration loading is expressed for each individual natural frequency f_D of a vibratory structure. This can be used to assess and compare loads and consequently to derive simplified damage-equivalent loads having an identical fatigue damage potential, i.e. the same FDS.

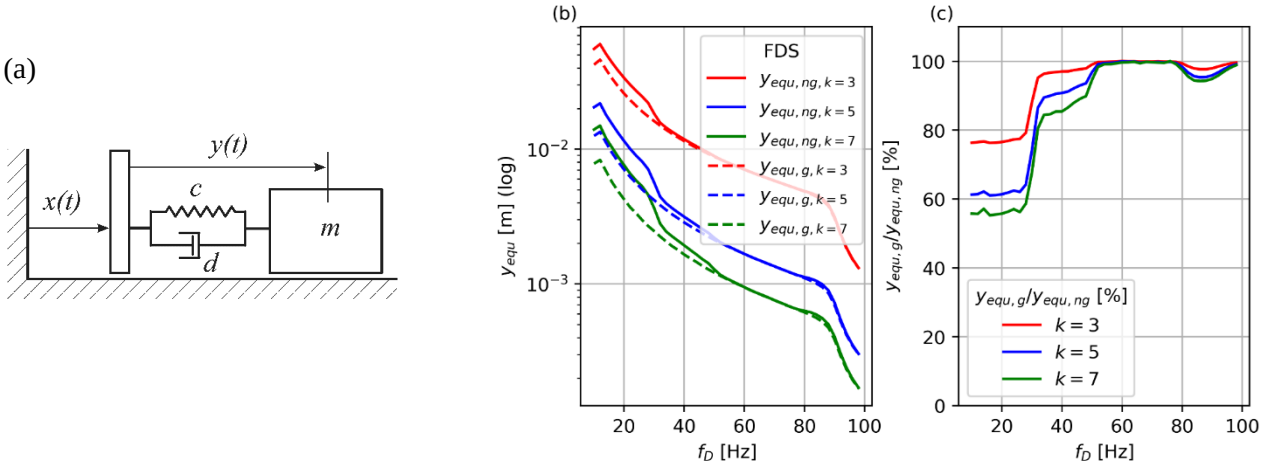

Figure 2: Fatigue Damage Spectrum (FDS). (a) SDOF model; (b) FDS $y_{\mathrm{equ},g}(f_D)$ and $y_{\mathrm{equ},ng}(f_D)$ for excitation signals $x_g(t)$ and $x_{ng}(t)$ for a damping ration of 3 % and different slope parameters k; (c) comparison of $y_{\mathrm{equ},g}(f_D)/y_{\mathrm{equ},ng}(f_D)$ in % of FDS of response signals $y_g(t)$ and $y_{ng}(t)$.

The corresponding model uses a single-degree-of-freedom (SDOF) vibratory system (Figure 2(a)) with mass m, spring c, damper d, acceleration excitation $x(t)$ and response displacement $y(t)$. Multiple resonant modes of real structures can be modelled by considering a parametrization with a variable natural frequency within a meaningful band and a damping ratio of a few percent. The displacement response $y(t)$ is assumed to be proportional to the deformation of a mode shape and consequently to the corresponding stress response $\sigma(t) = k_\sigma\, y(t)$. This might be conceived as the source of the fatigue damage of a corresponding vibratory structure. A subsequent application of a cycle-counting method (e.g. rainflow counting [27], here only range counting is applied, i.e. mean stresses are neglected) outputs a discrete load spectrum with J bins of cycle amplitudes $\sigma_j(n_j)$ (with: $j = 1 \ldots J$) and their corresponding counts n_j. By further considering a single slope S-N-curve (with slope parameter k in a log-log-plot and a reference point $\sigma_f(N_f)$) and a linear damage accumulation hypothesis (Palmgren-Miner-rule), the accumulated damage D can be derived as [27]:

$$N_f\, \sigma_f^k = N_j\, \sigma_j^k\ ; \qquad D = \sum_j \frac{n_j}{N_j} = \underbrace{\frac{k_\sigma^k}{N_f\, \sigma_f^k}}_{k_f} \sum_j n_j\, y_j^k \tag{4}$$

Since the main objective of the presented study is a comparison of different loads, the constant factor k_f is not relevant here. Consequently, to simplify the presentation, an equivalent load y_{equ} will be used:

$$y_{\mathrm{equ}} = \left(\sum_j n_j\, y_j^k\right)^{\frac{1}{k}} \tag{5}$$

Figure 2(b) shows the equivalent fatigue loads $y_{\mathrm{equ},g}(f_D)$ and $y_{\mathrm{equ},ng}(f_D)$ for the corresponding excitation signals $x_g(t)$ and $x_{ng}(t)$, resonant frequencies f_D from 5 Hz to 95 Hz, a damping ratio of 3 % and three common values of k. The comparison $(y_{\mathrm{equ,g}}(f_D)/y_{\mathrm{equ,ng}}(f_D)\ \cdot 100\ \%)$ is plotted in Fig. 2(b). It shows that the Gaussian assumption is clearly non-conservative for the fatigue damage of $y_{ng}(t)$. In addition the deviations of the damage results in the FDS are apparently related to the different degrees of non-stationarity of the frequency intervals $[10\ \mathrm{Hz}, 30\ \mathrm{Hz}]$, $[30\ \mathrm{Hz}, 50\ \mathrm{Hz}]$, $[50\ \mathrm{Hz}, 80\ \mathrm{Hz}]$ and $[80\ \mathrm{Hz}, 90\ \mathrm{Hz}]$ of the synthetic load $x_{ng}(t)$.

It is worth to mention here, that there are different mathematical procedures available for processing the required data numerically. The determination of the non-Gaussian response signals $y_{ng}(t)$ is possible either in the time domain based on i) a direct numerical integration of the differential equation describing the SDOF-model, ii) a numerical solution of the convolution integral using the impulse response function of the SDOF-model as well as in the frequency domain using iii) the transfer function $H_{xy}(f)$ of the SDOF-model and the Fourier-series representation of the input and output signals $X_{ng}(f)$ and $Y_{ng}(f) = H_{xy}(f)\, X_{ng}(f)$.

A subsequent application of cycle-counting algorithms provides the load spectra. Considerably less computational effort is needed in the case of Gaussian processes $x_g(t)$ and $y_g(t)$. Their PSDs $G_{xx}(f)$ and $G_{yy}(f)$ provide a full characterization of Gaussian processes, whereby they allow a major reduction of the number of required data points, as the PSDs are smooth functions for Gaussian processes. The calculation of the response uses the transfer function accordingly: $G_{yy}(f) = \left|H_{xy}(f)\right|^2 G_{xx}(f)$. Much faster PSD load cycle estimators can replace the above-mentioned time domain cycle-counting algorithm [28].

3 Derivation of stationary Gaussian fatigue equivalent load

As introduced there is no coherent theoretical foundation available for the description of non-Gaussian and non-stationary random vibration loads in the area of vibration fatigue. Therefore, a concise, comprehensive definition and comparison of loads is often hard to accomplish. Also the implementation of numerical and experimental fatigue analyses can be very challenging or even impossible due to limitations of computational power or hardware. However, for Gaussian stationary vibrations a very elegant and efficient PSD-based theory is available [28]. In addition, simulations and experiments can be conducted easily using the PSD-based load definitions. For this reason, it is very common to translate any kinds of loads into PSD-based signals having equivalent fatigue damage potentials. As introduced in Section 2.2 the FDS is a simple measure for describing the fatigue load potential of any kind of loads. Consequently it can be used for deriving fatigue-damage-equivalent PSD-based load descriptions for any kind of vibrational loads [14, 20–24]. The following Section 3.1 demonstrates this procedure for the derivation of a replacement PSD $G_{xx,\mathrm{re}}(f)$ based on the example signal $x_{ng}(t)$ introduced in Section 2.1 and discusses the open issues caused by the application of a specific damage hypothesis, which is actually a core part of the FDS concept. Subsequently Section 3.2 presents a solution to these issues based on the novel FDS approach using load spectra $y_j(n_j, f_D)$ instead of equivalent fatigue loads $y_{\mathrm{equ}}(f_D)$ for the FDS and of using a set of replacement PSDs $G_{xx,\mathrm{re},r}(f)$ (for: $r = 1 \ldots R$) instead of the usual single replacement PSD $G_{xx,\mathrm{re}}(f)$.

3.1 Approximation of FDS with a single Gaussian load

The numerical concept applied here for deriving a PSD-based replacement loads uses numerical optimization methods. The objective of such an optimization task is deriving single Gaussian-stationary replacement load signals $x_{g,\mathrm{re}}(t)$ by using its PSD description $G_{xx,\mathrm{re}}(f)$. The FDS $y_{\mathrm{equ,re}}(f_D)$ of s signal $x_{g,\mathrm{re}}(t)$ needs to be identical to the FDS $y_{\mathrm{equ},ng}(f_D)$ of the original excitation signal $x_{ng}(t)$. The objective function to minimize uses a least squares approach:

$$\sum_{n=1}^{N}\left[y_{\mathrm{equ},ng}(f_{D,n}, k) - y_{\mathrm{equ,re}}(f_{D,n}, k)\right]^2 \rightarrow \min \tag{6}$$

whereby $f_{D,n}$ stands for the individual natural frequencies where the FDS values are determined numerically (for: $n = 1 \ldots N$) and k stands for the corresponding slope parameter of the S-N-curve. The numerical representation of the replacement PSD $G_{xx,\mathrm{re}}(f)$ is based on the PSD $G_{xx,ng}(f)$ of the original signal $x_{ng}(t)$ scaled by the function $h(f)$:

$$G_{xx,\mathrm{re}}(f) = h(f)\, G_{xx,ng}(f) \tag{7}$$

For the numerical representation of the scaling function $h(f)$, an appropriate interpolation is used with data points f_i and $h_i(f_i)$ (for: $i = 1 \ldots I$) representing that function within the frequency interval given by $G_{xx,\mathrm{re}}(f)$. The final objective function to minimize is then:

$$\sum_{n=1}^{N}\left[y_{\mathrm{equ},ng}(f_{D,n}, k) - y_{\mathrm{equ,re}}(f_{D,n}, k, h_i)\right]^2 \rightarrow \min \tag{8}$$

with the I optimization variables h_i. The term $y_{\mathrm{equ,re}}(f_{D,n}, k, h_i)$ expresses the fact, that the I data points h_i of the scaling function $h(f)$ determine the approximation $y_{\mathrm{equ,re}}(f_{D,n}, k, h_i)$ of the FDS derived from $h(f)\, G_{xx,ng}(f)$; its numerical calculation comprises the steps presented in Section 2.2. It is worth to

mention, that the PSD-based procedure for calculating $y_{\mathrm{equ,re}}(f_{D,n}, k, h_i)$ constitutes an important detail for a fast and well converging numerical optimization. A robust starting point for the optimization is given by $h_i(f_i) = 1$ (corresponding to the FDS $y_{\mathrm{equ},g}(f_D, k)$ of the Gaussian signal $x_g(t)$).

Figure 3 depicts the results for three different values of $k = \{3, 5, 7\}$ and the underlying duration $T = 1000$ s of the original signal $x_{ng}(t)$. Figure 3(a) shows the replacement PSDs $G_{xx,\mathrm{re}}(f)$ for the different values of k as well as the original PSD $G_{xx,ng}(f)$. To clearly indicate the individual FDS-model used for the derivation, the slope parameter k is added to the notation: $G_{xx,\mathrm{re-3}}(f), G_{xx,\mathrm{re-5}}(f), G_{xx,\mathrm{re-7}}(f)$. From the FDS results given in Figure 2(c) it becomes clear, that the PSDs $G_{xx,\mathrm{re-k}}(f)$ have to have higher values than PSD $G_{xx,ng}(f)$ in the order $G_{xx,\mathrm{re-3}}(f) < G_{xx,\mathrm{re-5}}(f) < G_{xx,\mathrm{re-7}}(f)$. The comparison of $y_{\mathrm{equ,ng}}(f_D)$ and $y_{\mathrm{equ,re}}(f_D)$ for $k = \{3, 5, 7\}$ depicted in Figure 3(b) shows how the individual FDSs are successfully approximated by the procedure.

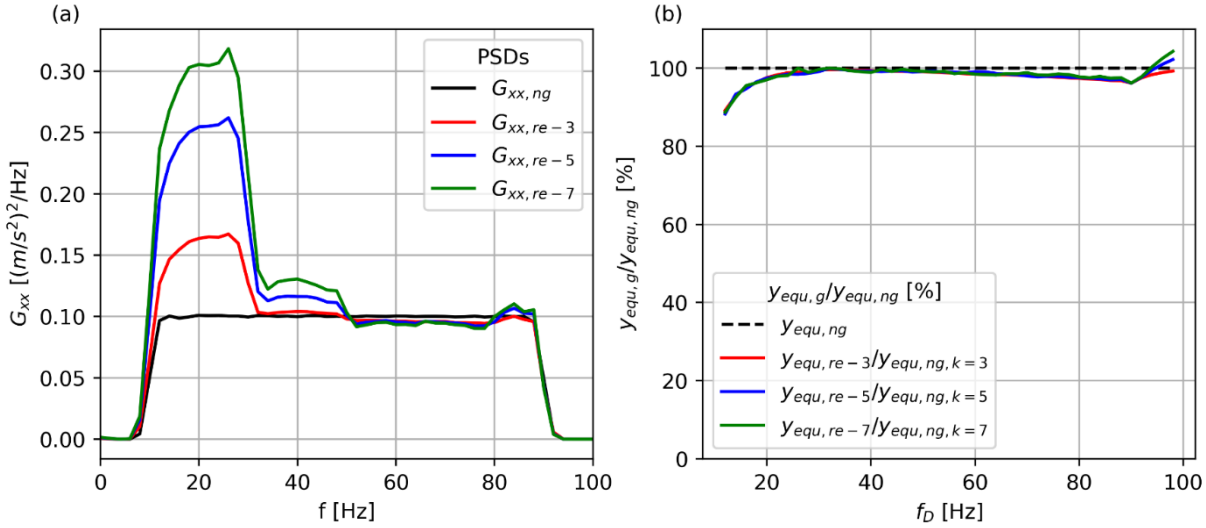

Figure 3: Gaussian replacement loads for different values of k. (a) PSD $G_{xx,ng}(f)$ of original non-Gaussian signal $x_{ng}(t)$ and PSDs $G_{xx,\mathrm{re-k}}(f)$ of replacement loads $x_{g,\mathrm{re-k}}(t)$ for $k = [3, 5, 7]$; (b) comparison of $y_{\mathrm{equ,re}}(f_D)/y_{\mathrm{equ,ng}}(f_D)$ in % of FDS of response signals $y_{g,\mathrm{re}}(t)$ and $y_{ng}(t)$.

The issue addressed by this paper is caused by the fact, that the derivation of the replacement loads $x_{g,\mathrm{re-k}}(t)$ is based on a specific fatigue damage model (here Palmgren-Miner rule with a given slope parameter k). If a certain fatigue damage model is used for that derivation, the resulting replacement loads $x_{g,\mathrm{re-k}}(t)$ will exclusively be valid for applications following that specific fatigue damage model. However, many real applications consist of component parts or assemblies contradicting this assumption. They comprise different S-N-curves with variable slopes, different materials with diverse surface qualities, notch characters, weld seams and so forth. For the example-data introduced above, this issue becomes obvious, if a replacement load $x_{g,\mathrm{re}}(t)$ derived for a specific value of k is applied to a problem actually having a different value k. Therefore, the data depicted in Figure 4 sensitizes for this issue: Figure 4(a) shows four different FDS curves $y_{\mathrm{equ}}(f_D, k)$ using $k = 7$ for the evaluation; one FDS-curve was calculated from the original signal $x_{ng}(t)$ and the remaining three were calculated from the replacement loads $x_{g,\mathrm{re-k}}(t)$, initially derived for $k = 3$, $k = 5$ and $k = 7$. As the deviations of these curves are hard to quantify within the FDS' log plot, Figure 4(b) shows in addition their comparison in percent. The results clearly show, that the analyzed case reveals a serious underestimation of the fatigue damage loads for the replacement loads with $k = 3$ and $k = 5$ – even for a minor non-Gaussian signal with a kurtosis $\beta_{ng} = 4$. The higher the degree of non-stationarity initially assigned to the frequency intervals of $x_{ng}(t)$ the higher is the deviation in the corresponding FDS.

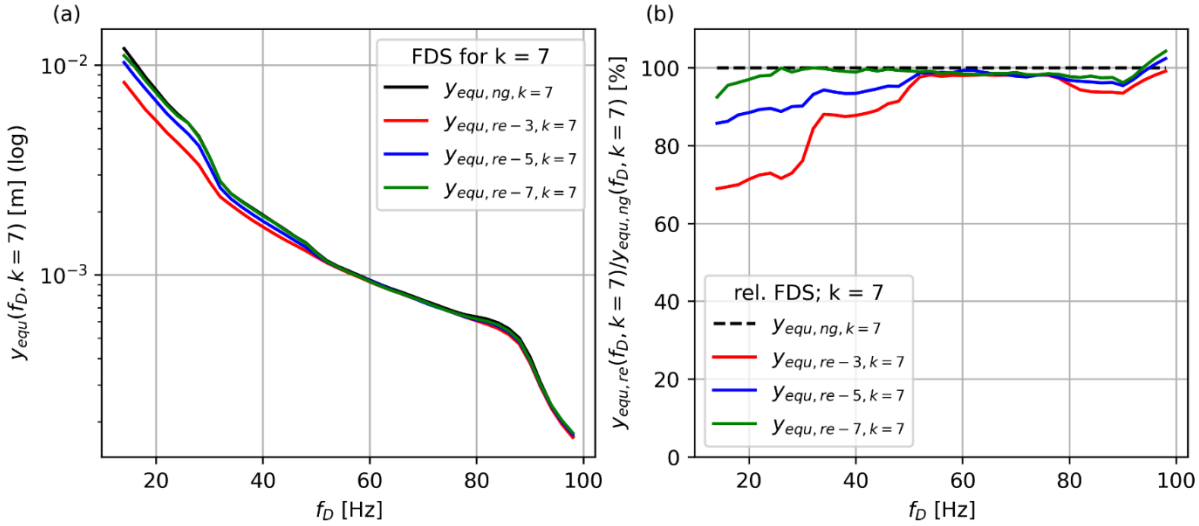

Figure 4: underestimation of fatigue damage caused by replacement loads $x_{g,\mathrm{re-k}}(t)$ originally derived with differing values of k. (a) FDS curves $y_{\mathrm{equ}}(f_D, k=7)$ using $k=7$ for the evaluation derived from i) signal $x_{ng}(t)$, ii-iv) replacement signals $x_{g,\mathrm{re-k}}(t)$ initially derived for $k=3$, $k=5$ and $k=7$; (b) comparison of curves from (a) in %.

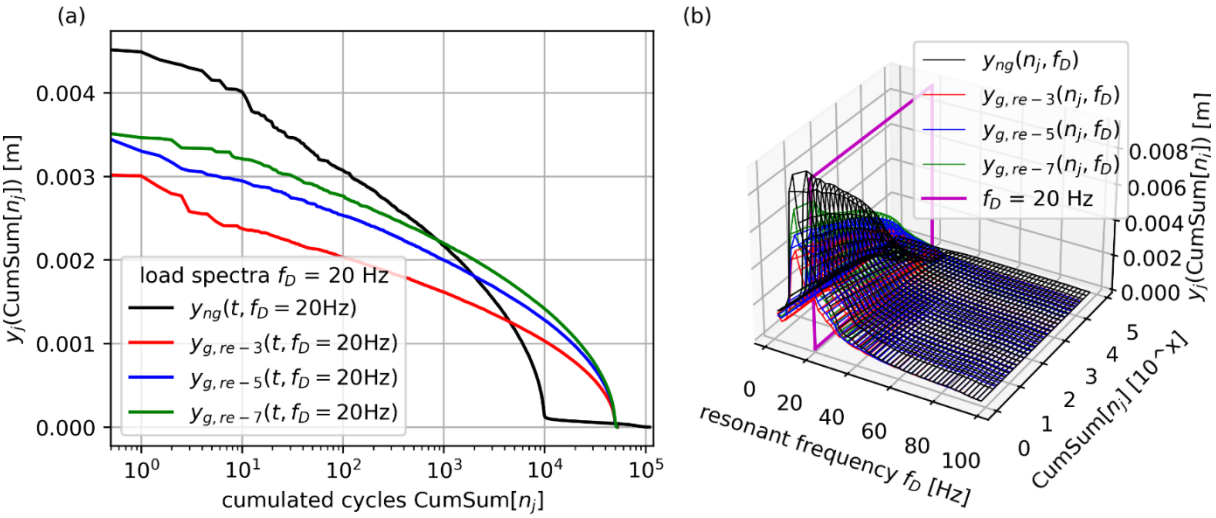

Figure 5: load spectra deviation caused by replacement loads $x_{g,\mathrm{re}}(t)$. (a) load spectra (load cycles $y_j(n_j)$ over cumulative number of load cycles n_j) of response $y_{ng}(t)$ induced by original excitation $x_{ng}(t)$ and the corresponding replacement loads $x_{g,\mathrm{re-3}}(t), x_{g,\mathrm{re-5}}(t), x_{g,\mathrm{re-7}}(t)$ initially derived for $k=3$, $k=5$ and $k=7$ for one certain natural frequency of $f_D = 20$ Hz; (b) representation of different load spectra for the full frequency range of the FDS.

These deviations are caused by the logic of the FDS, which reduces the vibration response $y(t)$ at the different natural frequencies f_D to corresponding equivalent fatigue damage values $y_{\mathrm{equ}}(f_D)$ by using a fatigue damage hypothesis expressed by a slope parameter k. A look at the corresponding load spectra $y_j(n_j)$ of these responses $y(t)$ reveals the problem behind the replacement loads. Figure 5(a) shows these load spectra at a certain unique frequency $f_D = 20$ Hz of the FDS; it compares the load spectra of the vibration response $y_{ng}(t)$ induced by the original excitation signal $x_{ng}(t)$ to the load spectra induced by the corresponding replacement signals $x_{g,\mathrm{re-3}}(t), x_{g,\mathrm{re-5}}(t), x_{g,\mathrm{re-7}}(t)$ initially derived for $k=3$, $k=5$

and $k = 7$. The different load spectra of $y_{g,\mathrm{re-k}}(t)$ are a clear indication for the procedure's sensitivity to the slope exponent. Further, Figure 5(b) highlights the fact that the extended FDS consists of individual load spectra for each natural frequency f_D. A solution to this issue is presented in the next Section; it is based on the idea of approximating not only the single equivalent fatigue damage values $y_{\mathrm{equ}}(f_D)$ at the different frequencies f_D, but the full response load spectra $y_j(n_j, f_D)$ at these frequencies f_D.

3.2 Approximation of extended FDS with multiple Gaussian loads

The limitation of the approach presented in the last Section 3.1 is caused by the fact, that the fatigue damage impact of a non-stationary and non-Gaussian excitation load $x_{ng}(t)$ is approximated by a single stationary Gaussian load $x_{g,\mathrm{re}}(t)$ (see Figure 5). This restrictive constraint makes it hard to achieve a satisfactory universal fatigue damage approximation, since the associated response load spectra are inherently inflexible. The proposals of the presented paper for a better solution are i) to use a set of R Gaussian loads $x_{g,\mathrm{re},r}(t)$ (for: $r = 1 \ldots R$) with different PSDs and durations T_r (with: $T = \sum_r T_r$) as a replacement load:

$$x_{g,\mathrm{re}}(t) = \begin{cases} x_{g,\mathrm{re},1}(t) & \text{for:} \quad 0 \quad \leq \; t \; \leq \quad T_1 \\ x_{g,\mathrm{re},2}(t) & \text{for:} \quad T_1 \quad < \; t \; \leq \quad T_1 + T_2 \\ \quad \vdots & \qquad\qquad < \; t \; \leq \\ x_{g,\mathrm{re},R}(t) & \text{for:} \quad T - T_R \; < \; t \; \leq \quad T \end{cases} \tag{9}$$

and ii) to approximate the load spectra $y_j(n_j)$ of the response signals $y_{g,\mathrm{re}}(t)$ at all the natural frequencies f_D of the SDOF system underlying the FDS. The idea of obtaining an approximation using multiple different Gaussian signals (quasi-stationary loading) to a non-Gaussian and non-stationary signal has already been analyzed before in different sources [11–13, 25, 26]. It contributes to the fact that real loading is regularly composed of various dominating load states. The idea of expressing that approximation by extending the FDS logic to load spectra is new to the knowledge of the authors.

Similar to the approximation by a single Gaussian load (Section 3.1) the numerical implementation is based on optimization techniques. The objective of this optimization is the derivation of multiple Gaussian-stationary replacement signal $x_{g,\mathrm{re},r}(t)$ (with: $r = 1 \ldots R$) with durations T_r and a corresponding PSD definition $G_{xx,\mathrm{re},r}(f)$. The representation of these PSDs adopts $G_{xx,ng}(f)$ of the original signal $x_{ng}(t)$ which is scaled by functions $h_r(f)$:

$$G_{xx,\mathrm{re},r}(f) = \; h_r(f)\, G_{xx,ng}(f); \qquad \text{with: } r = 1 \ldots R \tag{10}$$

The numerical representation of the scaling functions $h_r(f)$ is again implemented via an interpolation with data points f_i and $h_{r,i}(f_i)$ (for: $i = 1 \ldots I$), see corresponding approach in Section 3.1. The load spectra $y_{g,\mathrm{re},r_j}(n_{r_j})$ of the R Gaussian responses $y_{g,\mathrm{re},r}(f_{D,n}, t)$ at the N different natural frequencies $f_{D,n}$ of the SDOF system have to be accumulated to a total load spectrum for each frequency $f_{D,n}$:

$$n_j\left(y_{g,\mathrm{re}_j}, f_{D,n}\right) = \sum_{r=1}^{R} n_{r_j}\left(y_{g,\mathrm{re},r_j}, f_{D,n}\right) \tag{11}$$

All these individual load spectra at the N frequencies $f_{D,n}$ need to be identical to the corresponding response load spectra $y_{ng_j}(n_j)$ of the original excitation signal $x_{ng}(t)$. Therefore, equivalent to Eq. (7) the total objective function to minimize uses a least squares approach:

$$\sum_{n=1}^{N}\left\{\sum_{j=1}^{J}\left[y_{g,\mathrm{re}_j}(n_j, f_{D,n}) - y_{ng_j}(n_j, f_{D,n})\right]^2\right\} \rightarrow \min \tag{12}$$

with the additional constraint condition, that the total duration of the set of replacement signals corresponds to the duration of the original signal:

$$T = \sum_{r=1}^{R} T_r \tag{13}$$

The optimization variables are the $R \cdot I$ discrete data points of the R scaling functions $h_{r,i}(f_i)$ and the R durations T_r. The use of the above-mentioned PSD based numerical implementation is essential for a fast computation and also good convergence properties. The number R of replacement PSDs has to be determined in a way that it gives good approximations result for the underlying load spectra. As stated before a robust starting point for the optimization is given by $h_{r,i}(f_i) = 1$; for the durations $T_r = T/R$ works well.

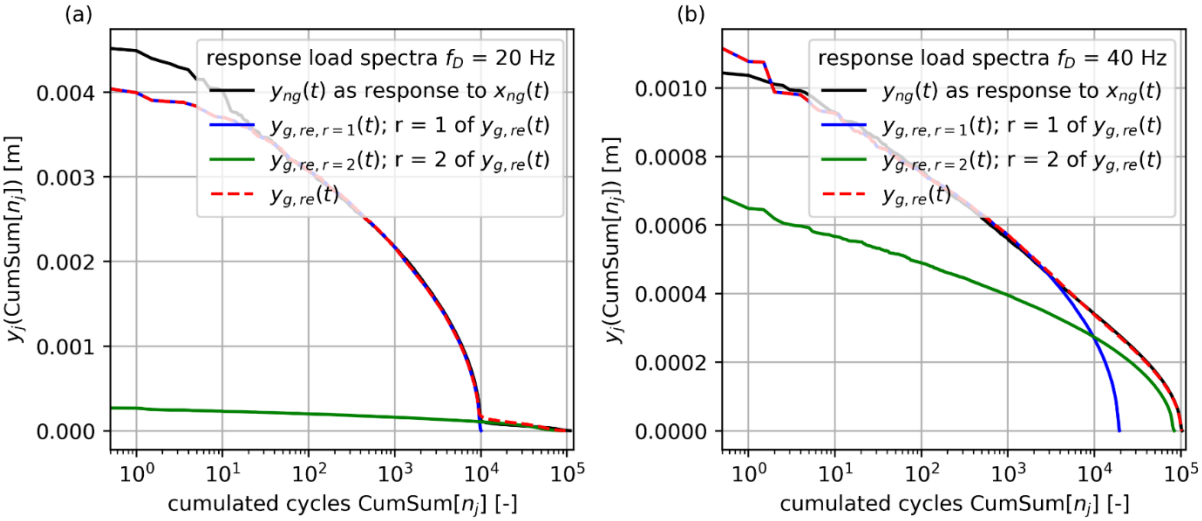

Figure 6: approximation of load spectra of response $y_{ng}(t)$ (load cycles $y_j(n_j)$ over cumulative number of load cycles n_j) induced by original excitation $x_{ng}(t)$ by two replacement loads $x_{g,\mathrm{re},r}(t)$ for the two single natural frequencies $f_D = 20$ Hz (a) and $f_D = 40$ Hz (b).

Figure 6 shows the results achieved with that procedure for the underlying quasi-stationary example for two selected frequencies of $f_D = 20$ Hz (6a) and $f_D = 40$ Hz (6b). Because of the initial definition of the quasi-stationary signal $x_{ng}(t)$ consisting of two stationary segments (see Section 2.1) a value of $R = 2$ was taken for the approximation. Each plot shows the corresponding load spectra of both segments $y_{g,\mathrm{re},r}(t)$, the respective total load spectrum of $y_{g,\mathrm{re}}(t)$ and also the load spectrum of the response $y_{ng}(t)$ induced by the original excitation signal $x_{ng}(t)$. In comparison to Figure 5(a) the deviations in the load spectra were successfully minimized by the new approach. Figure 7 shows the corresponding PSDs $G_{xx,\mathrm{re},r}(f)$ in (a) and the related time realizations $x_{g,\mathrm{re},r}(t)$ in (c). The PSDs $G_{xx,\mathrm{re},1}(f)$ and $G_{xx,\mathrm{re},2}(f)$ resulting from the optimization show a clear similarity to the PSDs $G_{xx,1}(f)$ and $G_{xx,2}(f)$ (see Figure 1a) initially used for the definition of signal $x_{ng}(t)$; even the solution of the corresponding durations T_r is close to the initial definition. To prove the advantages of the new approach the set of two piecewise stationary replacement signals $x_{g,\mathrm{re},1}(t)$ and $x_{g,\mathrm{re},2}(t)$ was subject to an FDS-based assessment and a comparison with the related FDS of the original signal $y_{ng}(t)$ was performed. The results are summarized in Figure 8 for the prior slope parameters $k = \{3, 5, 7\}$. In relation to Figure 2(b) and (c) the advantages are obvious: the FDS assessment of the replacement signals $x_{g,\mathrm{re},r}(t)$ is i) very close to the original signal $x_{ng}(t)$ and ii) independent of the value of k, resp. in general independent of a specific damage hypothesis. This is due to principal approach presented herein, using a load spectra based FDS method in conjunction with a set of piecewise stationary and Gaussian replacement loads.

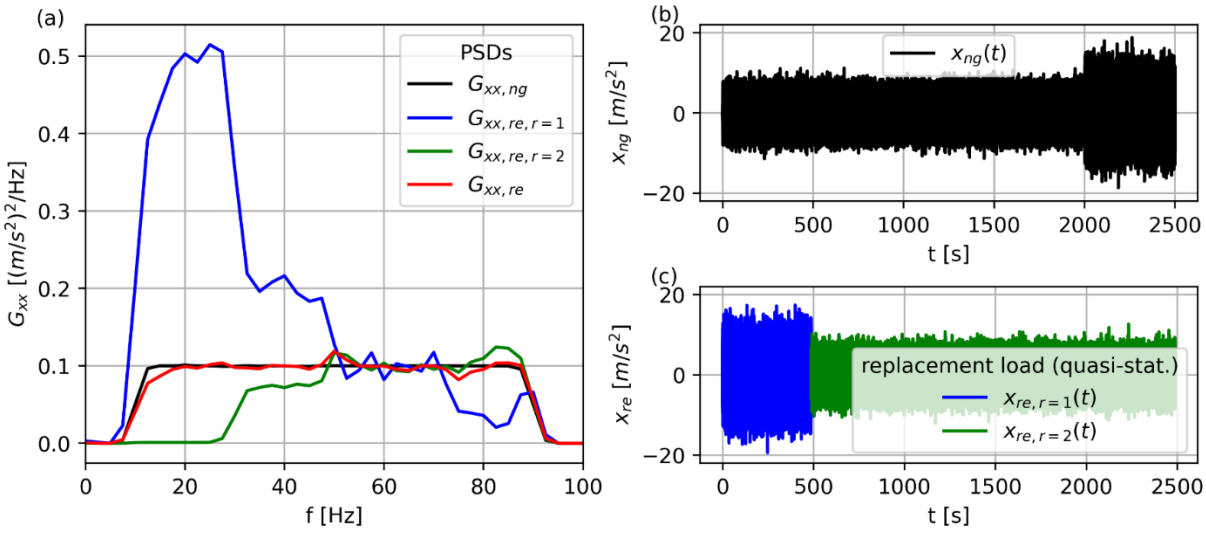

Figure 7: two replacement loads $x_{g,\mathrm{re},r}(t)$. (a) PSDs of original non-stationary, non-Gaussian signal $G_{xx,ng}(f)$, of $R = 2$ replacement loads $G_{xx,\mathrm{re},r}(f)$ and of total replacement load $G_{xx,\mathrm{re}}(f)$; (b) original signal $x_{ng}(t)$ from Figure 1(e); (c) representation of signals $x_{g,\mathrm{re},r}(t)$ from (a) in time domain.

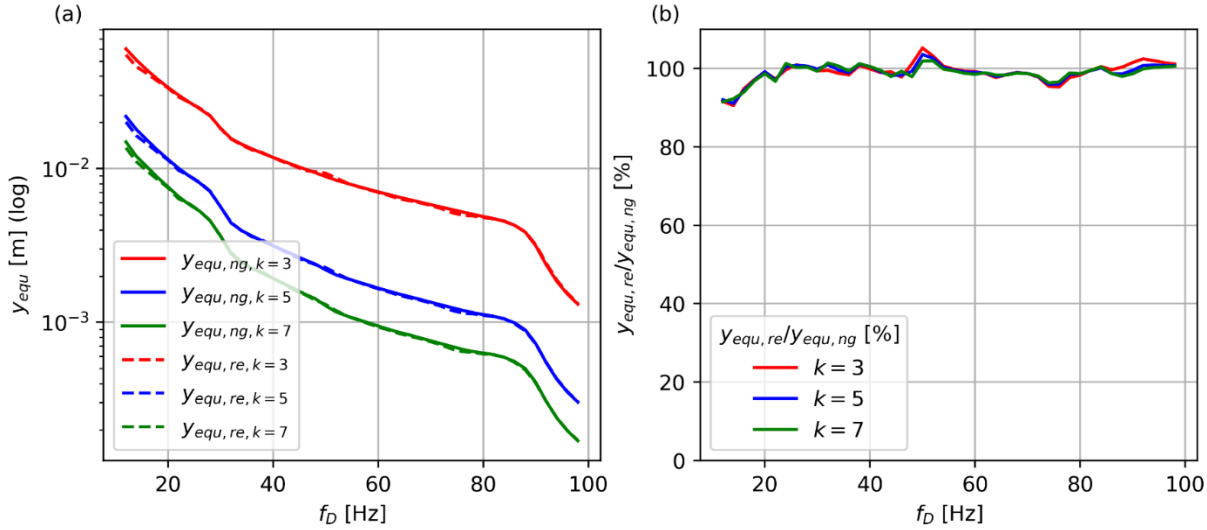

Figure 8: FDS of multiple replacement loads $x_{g,\mathrm{re},r}(t)$. (a) FDS curves $y_{\mathrm{equ}}(f_D)$ using $k = \{3, 5, 7\}$ for the synthetic signal $x_{ng}(t)$ and the set of piecewise stationary signals $x_{g,\mathrm{re},r}(t)$; (b) comparison of curves in (a) in percent.

4 Application to real data

The presentation in Sections 2 and 3 is based on a synthetically generated, non-stationary and non-Gaussian signal. A basic idea of using these synthetic signals is to make these reproducible. As the analysis of complex real loads with high kurtosis values might be more interesting and revealing, the current Section has the objective of applying the proposed method to recorded loading. The following example originating from a railway application demonstrates a broader validation of the proposed method. The corresponding excitation signal $x_{ng}(t)$ embodies the acceleration in vertical direction recorded at an axle box of a railway vehicle [25]. Figure 9(a) shows the signal with a total length of about $T = 1200$ s. Figure 9(b) depicts the PDF $p(x_{ng})$ and the corresponding Gaussian PDF $p_g(x)$ with same standard deviation σ. The kurtosis $\beta_{ng} = 29.25$ indicates a strong deviation from the Gaussian distribution. Using the proposed method, a set of

piecewise stationary Gaussian replacement loads were derived with a number of $R = 6$ to achieve a sufficient approximation, see Figure 9(c). Figure 9(b) also shoes the total PDF $p(x_{re})$ of the replacement signal and the corresponding kurtosis $\beta_{re} = 33.96$. To enable an assessment of the quality of the replacement signal, Figure 10 summarizes the results as presented before in Figure 8 for the synthetic signal $x_{ng}(t)$. Additionally, also the FDS curves $y_{\mathrm{equ,g}}(f_d)$ of the corresponding Gaussian process $x_g(t)$ are depicted, making the strong deviation of the fatigue potential obvious. Finally, Figure 11 represents the achieved result in relation to the load spectra of the response signals induced by the six replacement loads segments $x_{g,\mathrm{re},r}(t)$ for the selected frequencies of $f_D = 25$ Hz (11a), $f_D = 50$ Hz (11b), $f_D = 75$ Hz (11c) and $f_D = 100$ Hz (11d). The results clearly demonstrate that the initial objectives of i) replacing a non-stationary and non-Gaussian signal by a quasi-stationary Gaussian replacement signal having the same fatigue potential and ii) being independent of a specific fatigue damage hypothesis are achieved with success.

5 Conclusions

The presented paper introduced an extended Fatigue Damage Spectrum (FDS) using response load spectra as a fatigue damage measure for non-stationary and non-Gaussian random vibration loads. The new approach proved useful for the derivation of fatigue equivalent quasi-stationary Gaussian loads replacing non-Gaussian loads caused by an underlying modulation process evolving in time and frequency. As a definition of random vibratory signals based on stationarity and Gaussianity has major advantages for numerical and experimental fatigue analyses, the proposed method opens up new a new path for the solution of random vibration problems. It replaces a non-stationary, non-Gaussian load by a sequence of stationary Gaussian loads.

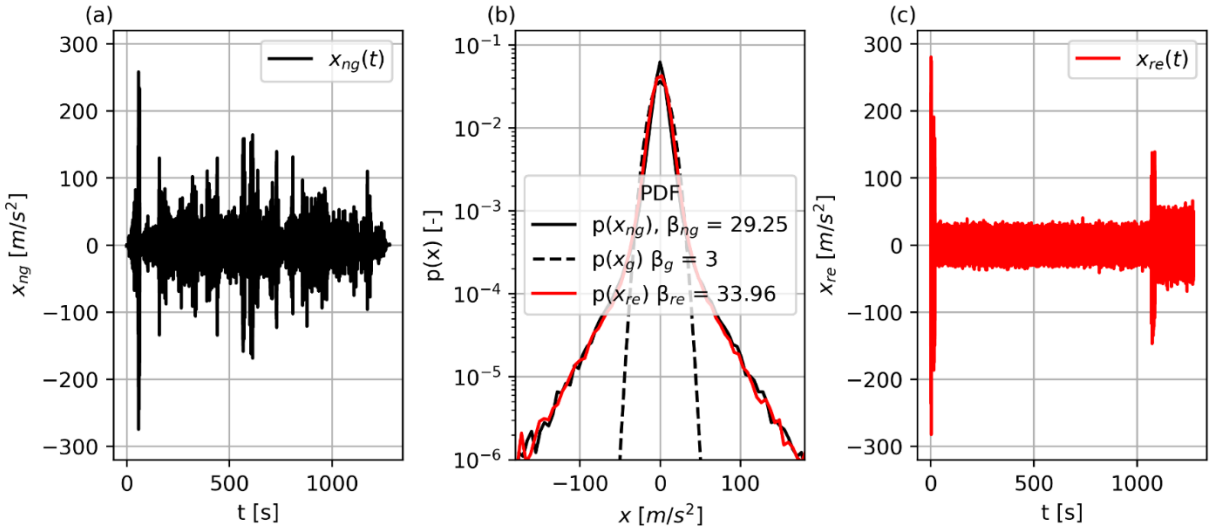

Figure 9: measured non-stationary and non-Gaussian acceleration signal from an axle box of a railway vehicle [25]. (a) time signal $x_{ng}(t)$; (b) PDFs of $x_{ng}(t)$, $x_{g,\mathrm{re}}(t)$ and corresponding Gaussian PDF; (c) quasi-stationary replacement signal $x_{g,\mathrm{re}}(t)$ consisting of $R = 6$ stationary parts $x_{g,\mathrm{re},r}(t)$.

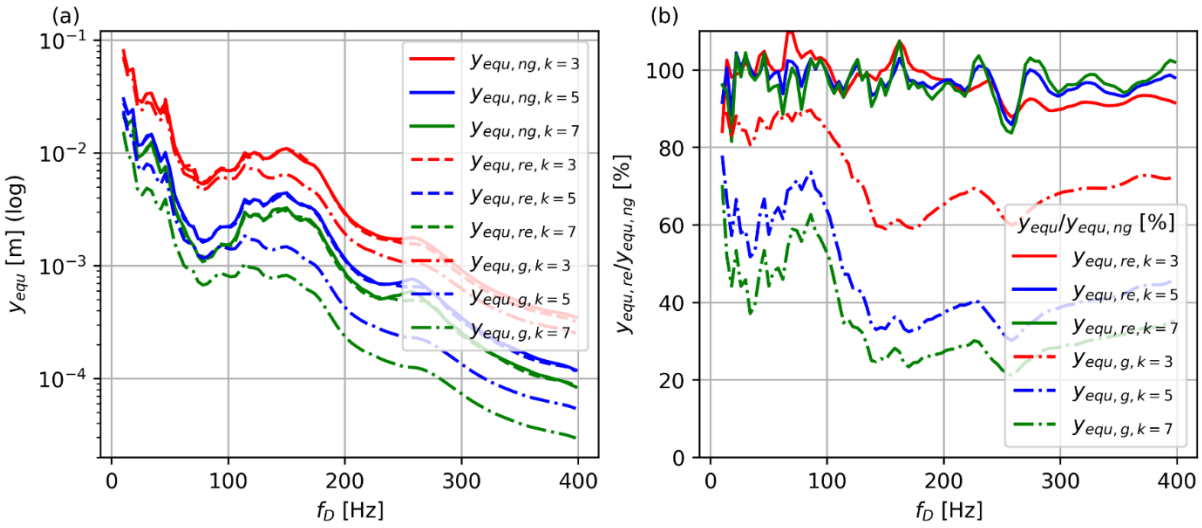

Figure 10: FDS of replacement loads $x_{g,\mathrm{re}}(t)$. (a) FDS curves $y_{\mathrm{equ}}(f_D)$ using $k = \{3, 5, 7\}$ for the recorded load $x_{ng}(t)$, the replacement load $x_{g,\mathrm{re}}(t)$ and the corresponding Gaussian load $x_g(t)$; (b) comparison of curves in (a).

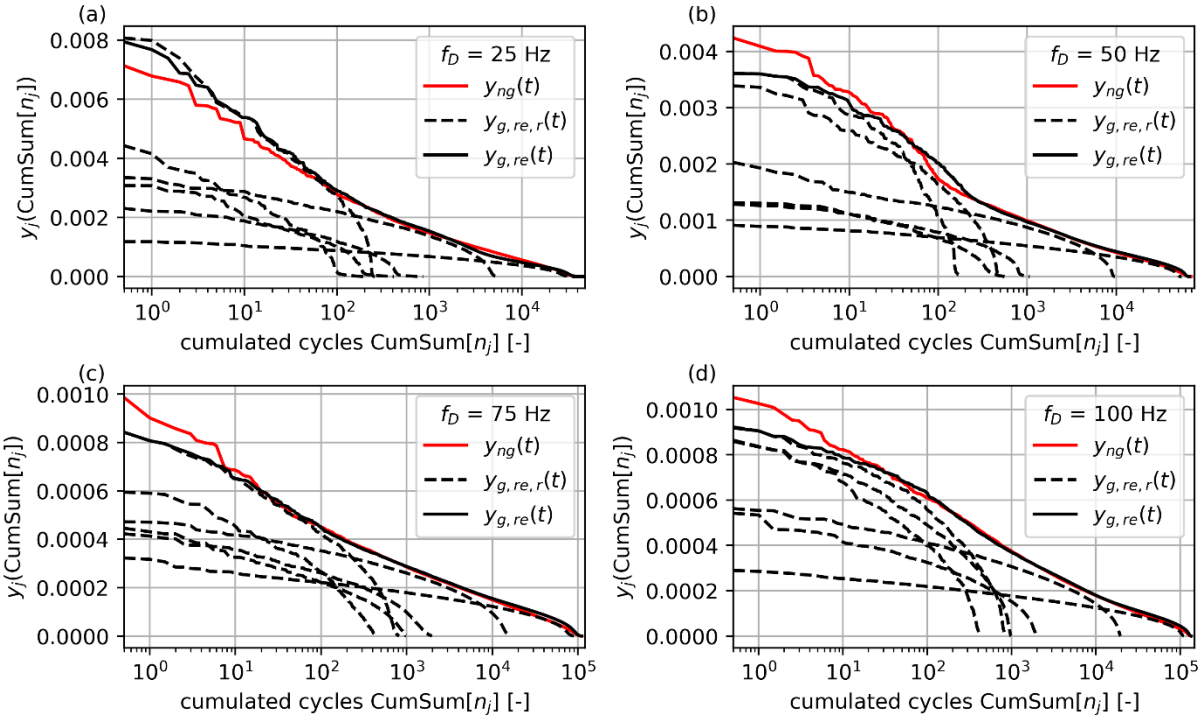

Figure 11: approximation of load spectrum of response $y_{ng}(t)$ (load cycles $y_j(n_j)$ over cumulative number of load cycles n_j) induced by original excitation $x_{ng}(t)$, total replacement load $x_{g,\mathrm{re}}(t)$ and set of 6 replacement loads $x_{g,\mathrm{re},r}(t)$ for four different natural frequencies $f_D = 25$ Hz (a), $f_D = 50$ Hz (b), $f_D = 75$ Hz (c) and $f_D = 100$ Hz (d).

Acknowledgements

Siemens AG Graz provided the analyzed measurements.

References

[1] D. Benasciutti, and R. Tovo, "Fatigue life assessment in non-Gaussian random loadings," *International Journal of Fatigue*, vol. 28, no.. 7, pp. 733–746, 2006.

[2] F. Cianetti, M. Palmieri, C. Braccesi, and G. Morettini, "Correction formula approach to evaluate fatigue damage induced by non-Gaussian stress state," *Procedia Struct. Int.* 8, 2018, pp. 390–398.

[3] A. Steinwolf, "Analysis and approximation of probability distribution of vehicle random vibration with consideration of kurtosis and skewness values," in *Structural dynamics: recent advances*, 1994, pp. 785–794.

[4] D. O. Smallwood, "Generating Non-Gaussian Vibration for Testing Purposes, : Dynamic Testing. Dynamic Testing," *Sound and Vibration Magzine*, vol. 39, no. 10, pp. 18–23, 2005.

[5] S. R. Winterstein, "Nonlinear Vibration Models for Extremes and Fatigue," *Journal of Engineering Mechanics*, vol. 114, no. 10, pp. 1772–1790, 1988.

[6] Z. Li, and A. Ince, "A unified frequency domain fatigue damage modeling approach for random-on-random spectrum," *International Journal of Fatigue*, vol. 124, pp. 123–137, 2019.

[7] A. Trapp, J. M. Mafake, and P. Wolfsteiner, "Fatigue assessment of amplitude-modulated non-stationary random vibration loading," *Procedia Structural Integrity*, vol. 17, pp. 379–386, 2019.

[8] M. Palmieri, M. Cesnik, J. Slavic, F. Cianetti, and M. Boltezar, "Non-Gaussianity and non-stationarity in vibration fatigue," *International Journal of Fatigue*, vol. 97, pp. 9–19, 2017.

[9] A. Trapp, and P. Wolfsteiner, "Characterizing non-Gaussian vibration loading using the trispectrum," *Journal of Physics: Conference Series* vol. 1264, 2019.

[10] A. Trapp, F. Hollweck and P. Wolfsteiner, "On the transmission of non-Gaussian random loading through linear structures," In: *Moreira, P. M. G. P; TAVARES, P. J. S. (Hrsg.): The 4th International Conference on Structural Integrity* : *ICSI 2021*, 2021.

[11] A. Trapp, and P. Wolfsteiner, "Estimating higher-order spectra via filtering-averaging," *Mechanical Systems and Signal Processing*, vol. 150, 2021.

[12] A. Trapp, and P. Wolfsteiner, "Frequency-domain characterization of varying random vibration loading by a non-stationarity matrix," *International Journal of Fatigue*, vol. 146, 2021.

[13] A. Trapp, and P. Wolfsteiner, "Fatigue assessment of non-stationary random loading in the frequency domain by a quasi-stationary Gaussian approximation," *International Journal of Fatigue*, vol. 148, 2021.

[14] C. Lalanne, *Mechanical vibration and shock analysis*. 2nd ed. London, Hoboken N.J. : ISTE; Wiley, 2009.

[15] J. Zhang, K. Chen, J. Shen, G. Yang, C. Liu and Y. Fu, "Accelerated Vibration Durability Test Analysis of Aviation Equipment Based on Different Fatigue Damage Spectrum Calculation Methods," in *2020 11th International Conference on Prognostics and System Health Management (PHM-2020 Jinan)* : IEEE, 2020, pp. 401–407.

[16] A. Angeli, B. Cornelis, and M. Troncossi, "Synthesis of Sine-on-Random vibration profiles for accelerated life tests based on fatigue damage spectrum equivalence," *Mechanical Systems and Signal Processing*, vol. 10, pp. 340–351, 2018.

[17] F. Cianetti, A. Alvino, A. Bolognini, M. Palmieri, and C. Braccesi, "The design of durability tests by fatigue damage spectrum approach," *Fatigue & Fracture of Engineering Materials & Structures*, vol. 41, no. 4, pp. 787–796, 2018.

[18] J. van Baren, "Fatigue Damage Spectrum – A New Tool to Accelerate Vibration Testing," *Sound&Vibration*, vol. 15, 2015.

[19] P. Wolfsteiner, and A. Trapp, "Fatigue life due to non-Gaussian excitation – An analysis of the Fatigue Damage Spectrum using Higher Order Spectra," *International Journal of Fatigue*, vol. 127, pp. 203–216, 2019.

[20] MIL-STD-810G w/Change 1. 2014. *Environmental Engineering Considerations and Laboratory Tests*

[21] S. McNeill, "Implementing the Fatigue Damage Spectrum and Fatigue Damage Equivalent Vibration," in *proceedings of the 79th Shock and Vibration Symposium*, 2008, pp. 1–20.

[22] J. Jang, and J.-W. Park, "Simplified Vibration PSD Synthesis Method for MIL-STD-810," *Applied Sciences*, vol. 10, no. 2, pp. 458, 2020

[23] M. Decker, S. Kinscherf, N. Bauer, P. David, and M. Serifsoy, "Deriving fatigue equivalent power spectral density spectra for the vibration testing of engine components," *Materialwissenschaft und Werkstofftechnik*, vol. 49, no. 3, pp. 392–405, 2018.

[24] M. Decker "Vibration fatigue analysis using response spectra," *International Journal of Fatigue*, vol. 148, pp. 106192, 2021

[25] P. Wolfsteiner, "Fatigue assessment of non-stationary random vibrations by using decomposition in Gaussian portions," *International Journal of Mechanical Sciences*, vol. 127, pp. 10–22, 2017.

[26] V. Rouillard, and M. A. Sek, "Synthesizing nonstationary, non-Gaussian random vibrations," *Packaging Technology and Science*, vol. 23, no. 8, pp. 423–439, 2010.

[27] E. Haibach, *Betriebsfestigkeit* : *Verfahren und Daten zur Bauteilberechnung*. 3., korrigierte und erg. Aufl. Berlin : Springer, 2006 (VDI-Buch)

[28] M. Mrsnik, J. Slavic, and M. Boltezar, "Frequency-domain methods for a vibration-fatigue-life estimation – Application to real data," *International Journal of Fatigue*, vol. 47, pp. 8–17, 2013.

Appendix

A Nomenclature

c	spring stiffness
d	damper constant
f, f_D	frequency , natural frequency
$h(f)$	scaling function
$h_i(f_i)$	data points of scaling function
$h_{r,i}(f_i)$	data points of scaling function for Gaussian signal r
i	index of interpolation data points
j	index of cycle classes
k	slope parameter of damage hypothesis
k_σ, k_f	stress constant
m	mass
m_n	n-th statistical moment
n	index of FDS frequencies
n_j	Number of cycles in class j
$p(x)$	PDF of $x(t)$
r	index of replacement PSDs
$x(t)$	realization of random process $X(t)$, excitation signal
$x_g(t)$	Gaussian excitation signal
$x_{ng}(t)$	non-Gaussian excitation signal
$x_{g,\mathrm{re}}(t)$	Gaussian replacement signal for $x_{ng}(t)$
$x_{g,\mathrm{re-k}}(t)$	Gaussian replacement signal for $x_{ng}(t)$ derived with slope parameter k
$x_{g,\mathrm{re},r}(t)$	r-th Gaussian replacement signal for $x_{ng}(t)$
$y(t)$	response signal
$y_g(t)$	Gaussian response signal
$y_{ng}(t)$	non-Gaussian response signal
y_{equ}	equivalent fatigue load
$y_{\mathrm{equ}}(f_D)$	FDS expressing the equivalent fatigue load
$y_{\mathrm{equ},g}(f_D)$	FDS expressing the equivalent fatigue load of a Gaussian signal
$y_{\mathrm{equ},ng}(f_D)$	FDS expressing the equivalent fatigue load of a non-Gaussian signal
$y_j(n_j, f_D)$	load spectrum of displacement bins y_j and cycle counts n_j at frequency f_D
D	accumulated damage
$G_{xx,g}(f)$	PSD of $x_g(t)$
$G_{xx,\mathrm{re}}(f)$	PSD of $x_{g,\mathrm{re}}(t)$

$G_{xx,\mathrm{re-k}}(f)$	PSD of $x_{g,\mathrm{re}-k}(t)$
$G_{xx,\mathrm{re},r}(f)$	PSD of $x_{g,\mathrm{re},r}(t)$
$G_{xx,ng}(f)$	PSD of $x_{ng}(t)$
$G_{yy,g}(f)$	PSD of $y_g(t)$
$G_{yy,ng}(f)$	PSD of $y_{ng}(t)$
$H_{xy}(f)$	transfer function
I	number of interpolation data points i
J	number of cycle classes j
N	number of FDS frequencies n
R	number of replacement PSDs r
T	duration
$X(t)$	random process
$X_{ng}(f)$	Fourier-series of $x_{ng}(t)$
$Y_{ng}(f)$	Fourier-series of $y_{ng}(t)$
β	kurtosis
μ_x	mean of $x(t)$
μ_n	n-th central statistical moment
σ	standard deviation
$\sigma(t)$	stress signal
$\sigma_j(n_j)$	load spectrum of stress bins σ_j and cycle counts n_j
$\sigma_f(N_f)$	reference point of wöhler-line